

This final rotation only changes the phase of  $\Psi_3$  and  $\Psi_4$  and hence cannot change the ultimate classification.

<sup>34</sup>H. Weyl, *The Theory of Groups and Quantum Mechan-*

*ics* (Dover, New York, 1931), Chap. III, Sec. 4. Weyl says "completely reducible" where we say "decomposable."

PHYSICAL REVIEW D

VOLUME 8, NUMBER 10

15 NOVEMBER 1973

## Experimental Search for Anisotropy in the Speed of Light\*†

William S. N. Trimmer,‡ Ralph F. Baierlein, James E. Faller,§ and Henry A. Hill||

*Wesleyan University, Middletown, Connecticut 06457*

(Received 9 April 1973)

A triangular interferometer passes two beams around the interferometer in opposite directions. A portion of the optical path contains a piece of glass. If the phase velocity of light is anisotropic, the fringe pattern will shift as the interferometer is rotated relative to the fixed stars. The interferometer is sensitive to anisotropies that behave as the first or third Legendre polynomials,  $P_1(\cos\phi)$  and  $P_3(\cos\phi)$ , where  $\phi$  is the angle between a preferred direction in space and the direction of light propagation. The maximum change in the speed of light is less than  $0.03 \pm 2.5$  cm/sec for the  $P_1$  anisotropy, and is less than  $0.7 \pm 0.45$  cm/sec for the  $P_3$  anisotropy. If an ether wind can be described by a Fresnel dragging coefficient when light passes through glass, the ether wind would be detectable by this experiment. This experiment sets an upper limit of  $0.045 \pm 3.8$  cm/sec for the ether wind at the surface of the earth. This is about one-millionth of the earth's orbital velocity.

### I. INTRODUCTION

A basic assumption of relativity theory is that, in an inertial frame, the speed of light is the same in all directions. Though the weight of experimental evidence can strongly support this assumption, such an assumption can never be proven true. The possibility always exists that there is an unthought-of anisotropy, or that the anisotropy lies below experimental error. This paper describes an interferometer used to search for several anisotropies.

Figure 1 shows the interferometer used. Light entering the interferometer from the light source is split by the beam splitter into two beams which travel around the interferometer in opposite directions. These two beams recombine on the beam splitter, and a fringe pattern is formed by the lens. When the glass is present, both beams pass through the glass. During data runs, the apparatus is rotated to different orientations. If a detectable anisotropy exists, the fringe pattern will shift as the interferometer is rotated.

Shifts of the fringe position are analyzed for anisotropies that behave as

$$\frac{1}{c(\phi)} = \frac{1}{c_0} [1 + b_1 P_1(\cos\phi) + b_3 P_3(\cos\phi)], \quad (1)$$

where

$$P_1(\cos\phi) = \cos\phi, \quad (2)$$

$$P_3(\cos\phi) = \frac{1}{2}(5\cos^3\phi - 3\cos\phi) \\ = \frac{1}{8}(5\cos 3\phi + 3\cos\phi). \quad (3)$$

In these expressions,  $c(\phi)$  is the vacuum phase velocity of light in a direction that makes an angle  $\phi$  with a presumed single preferred direction in space. The constant  $c_0$  is the average speed of light. The parameters  $b_1$  and  $b_3$  are small numbers which are a measure of the size of the anisotropy. Later it will be shown that the  $P_3$  anisotropy can be seen both with and without the glass being present in the interferometer, whereas the  $P_1$  anisotropy can be seen only when the glass is present. The use of the index of refraction to measure the  $P_1$  anisotropy will be discussed in Sec. II of this paper and also in Sec. II of the following paper.<sup>1</sup> The final results of this experiment will be expressed as upper limits on  $b_1$  and  $b_3$ .

### II. THEORY

The physical observable is the position of the fringe pattern. Since fringe shifts are caused by changes in the optical path length, one needs to

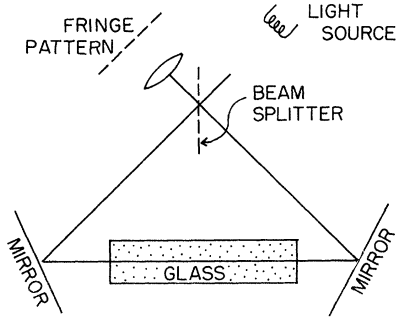


FIG. 1. A diagram of the interferometer used in this experiment.

examine the optical path length to determine what kinds of anisotropies can be detected.

For a monochromatic light beam, the optical path length ( $L_{o.p.}$ ) between two arbitrary points  $A$  and  $D$  on this path is

$$\begin{aligned} L_{o.p.} &= \text{number of wavelengths} \\ &\quad \text{contained between } A \text{ and } D \\ &= \int_A^D \lambda^{-1} dl. \end{aligned} \quad (4)$$

Here  $\lambda$  is the wavelength, and  $dl$  is the incremental path length. The fundamental relationship

$$\begin{aligned} \lambda \nu &= c(\phi) n^{-1} \\ &= \text{phase velocity}, \end{aligned} \quad (5)$$

where  $n$  is the index of refraction and  $\nu$  the frequency, enables one to write

$$L_{o.p.} = \int_A^D n \nu c_0^{-1} [1 + b_1 P_1(\cos \phi) + b_3 P_3(\cos \phi)] dl. \quad (6)$$

There are several interesting observations to be made about Eq. (6). First, if the frequency was different at different points along the optical path, there would be an accumulation of wavelengths between these points. That would be unreasonable and so it is assumed  $\nu$  is everywhere constant along a stationary optical path. This allows one to remove  $\nu$  from the integral in Eq. (6). Second, it will be assumed later in the analysis that the index of refraction at any given point in the optical path length is a constant,  $n$ , that depends upon only the properties of the material, not upon the direction in which the light is propagating. Under conditions less stringent than this, fringe shifts could still be

observed. This condition is discussed in Sec. II of the following paper.

First consider the anisotropy that behaves as  $P_1(\cos \phi) = \cos \phi$ . The optical path for this term is

$$L_{o.p.}(P_1) = \nu b_1 c_0^{-1} \int_A^D n \cos \phi dl. \quad (7)$$

For a closed optical path such as our interferometer, this term sums to zero unless there is a change in the refractive index along the path. If  $n$  is a constant over the whole path, it can be moved to the left of the integral. Then, as Fig. 2 shows,  $\cos \phi$  is the projection of the path length on the preferred direction, and for a closed path this sums to zero. If there is glass present in part of the path, however, the index of refraction can be written as  $n = 1$  for the nonglass portion of the path, and as  $n = 1 + g$  for the glass portion of the path. Typically,  $g$  is approximately  $\frac{1}{2}$ . The optical path can now be written as

$$L_{o.p.}(P_1) = \nu b_1 c_0^{-1} \left[ \int_A^D 1 \cos \phi dl + \int_B^C g \cos \phi dl \right], \quad (8)$$

where the integral over  $A$  to  $D$  is a closed path and  $B$  to  $C$  is the portion of the path containing the glass, as shown in Fig. 3. The first integral was shown to sum to zero. The second integral adds an extra optical path length which does not cancel with the rest of the path. It is this integral that makes the  $P_1$  anisotropy observable.

An anisotropy that behaves as  $P_3$  is observable both with and without the glass. It is straightforward to show this by writing out the optical path length for this case. Anisotropies that behave as  $P_{\text{even}}$  (the even Legendre polynomials) are not observable because our interferometer subtracts beams traveling in opposite directions, and the  $P_{\text{even}}$  anisotropies are identical for beams traveling

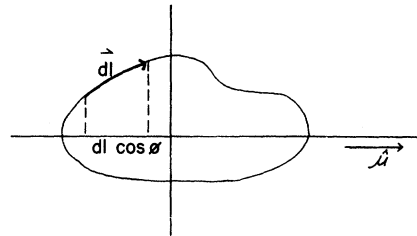


FIG. 2. Projection of an optical path on a preferred direction  $\hat{\mu}$ .

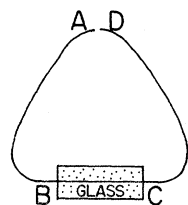


FIG. 3. The optical path described by Eq. (8).

in opposite directions. The Michelson-Morley interferometer, however, is sensitive to these  $P_{\text{even}}$  anisotropies. An analysis for anisotropies that behave as the Legendre polynomials of odd order higher than the third was not made. Such anisotropies would have required better knowledge of the exact orientation of the apparatus relative to the celestial sphere than was available experimentally.

### III. THE APPARATUS

The interferometer, illustrated in Fig. 1, is a triangular interferometer with interior angles  $45^\circ$ ,  $90^\circ$ ,  $45^\circ$ , and arm lengths of 12 cm, 17 cm, and 12 cm. The glass is 12 cm long and is made of crown glass with a refractive index of 1.5. The fringe pattern of an interferometer with these angles is less sensitive to small tips of the mirrors than most interferometers.<sup>2</sup> During the data runs, the plane defined by the normals to the mirrors (or alternately the plane of the light paths) is perpendicular to the local force of gravity. During the basic data-taking cycle of one minute, the average position of the fringe pattern is measured and then the apparatus is rotated  $60^\circ$  to the next data-taking position. Data are taken continuously once a minute for several days at a time.

The interferometer is mounted on a two-inch thick piece of aluminum jig plate and enclosed in a vacuum chamber. The chamber rotates on a carefully-leveled granite surface plate. In order to keep the bearings from crushing the granite surface plate, a thin piece of shim stock is used to separate them. The vacuum chamber is automatically rotated by a motor which is actuated by an on-line computer.

The detection electronics uses phase sensitive detection. A light-emitting diode driven at 160 hertz is used as the light source, and a white-light fringe pattern is produced by the interferometer. The light from either side of the white-light maximum is imaged on two separate detectors. An operational amplifier mounted on the interferometer base takes the difference current between these two detectors. The resultant output is a small 160-hertz signal, which comes out of the

rotating vacuum chamber via a long and flexible coaxial cable to a phase sensitive detector. The output of the phase sensitive detector is proportional to the 160-Hz difference signal, and hence to the fringe position. This output is digitally recorded and stored for analysis.

Because the detection electronics measures the center of a white-light fringe pattern, the experiment is insensitive to changes in the color of the light source. Hence even if the light was emitted from the light source with slightly different frequencies in different directions, this experiment would be insensitive to these frequency anisotropies, and a frequency anisotropy could not mask a velocity anisotropy. Another experiment has been performed to detect frequency anisotropies as a function of the direction in space the photons were emitted. This experiment used radioactive  $\text{Co}^{57}$  as a source of photons, and the frequency of the emitted photons was measured by detecting how many photons were transmitted through a natural iron absorber.<sup>3</sup>

### IV. DATA ANALYSIS

This section will discuss the assembling and analysis of the data, and the final numerical results.

A data set consists of data taken continuously (once a minute) for several days. These data are grouped according to which hour they were taken and the orientation of the apparatus. All of the data taken during one hour with the apparatus in a specific position are averaged together. The six different orientations of the apparatus give six averages for each hour. During the 24 hours of a day, 144 averages are accumulated. These 144 averages represent the data to be analyzed. If several days' data are used in an analysis, the same time and position averages from different days are averaged together, still giving 144 data averages. Two sets of data were used in the final analysis. One set was formed from three days of data acquisition with the glass present in the interferometer. The other set consisted of four days of continuous data taken with no glass in the interferometer.

Because the earth rotates 15 degrees during the time one hour average is taken, the true position of the apparatus relative to the celestial sphere is uncertain by a few degrees. The worst case degradation of the sensitivity of the apparatus due to this rotation is 5%. Because the data were accumulated over a period of five days, the difference between the sidereal day and the mean solar day is 20 minutes or  $5^\circ$ . This angle is small and can be neglected.

The data analysis performed is a least-squares fit between the 144 observed data points and the assumed form of the anisotropy. The theoretically calculated change in the fringe pattern, due to this assumed form, is  $(D_{th})_i$ . This number represents the difference between the two optical paths of the interferometer, and the first term of Eq. (6) cancels. When one includes a scale factor  $F$ ,  $(D_{th})_i$  becomes

$$(D_{th})_i = F \sum_{m=1}^3 [b_1 P_1(\cos \phi_i) + b_3 P_3(\cos \phi_i)] \int_{arm\ m} n\, dl. \quad (9)$$

Here  $i$  specifies the orientation of the apparatus, and  $b_1$  and  $b_3$  specify the assumed size of the anisotropies. The integral over  $n\,dl$  is the integral over arm  $m$  of the interferometer, where the sum  $m=1, 3$  includes all three arms of the interferometer. To perform a least-squares fit, one forms the variance

$$S = \sum_{i=1}^{144} [(D_{th})_i - (D_{exp})_i]^2, \quad (10)$$

and looks for those values of  $b_1, b_3$  and the presumed preferred direction which minimize  $S$ . In this expression,  $(D_{exp})_i$  is one of the 144 experimentally observed data points. The angle  $\phi$  is really an angle in three dimensions and must be expressed by two angles  $\psi$  and  $\xi$  that specify the preferred direction relative to the celestial sphere. One normally sets

$$\frac{\partial S}{\partial b_1} = 0, \quad (11a)$$

$$\frac{\partial S}{\partial b_3} = 0, \quad (11b)$$

$$\frac{\partial S}{\partial \psi} = 0, \quad (11c)$$

$$\frac{\partial S}{\partial \xi} = 0, \quad (11d)$$

which give four equations and four unknowns. However, the (11c) and (11d) equations are unmanageable. Therefore the (11a) and (11b) equations were solved analytically, and used to eliminate  $b_1$  and  $b_3$  from equations (11c) and (11d). Then, on a computer,  $S$  was calculated for a number of different angles  $\psi$  and  $\xi$ , and the direction yielding the minimum  $S$  was found. When the minimum  $S$  is found, the corresponding values of  $b_1, b_3, \psi$ , and  $\xi$  represent the best least-squares fit. To calibrate the sensitivity of the apparatus, a known anisotropy is added to the 144 data points, and the smallest added anisotropy that is observable over the noise of the data is the limit of sensitivity of

the apparatus.

The results of this experiment are expressed as a ratio: the maximum change in the speed-of-light attributable to an anisotropy, divided by the speed of light. This means that the quoted results are the best-fit value of the coefficients  $b_1$  and  $b_3$ . For anisotropies that behave as  $P_1$  this ratio is  $(0.1 \pm 8.4) \times 10^{-11}$ , and for  $P_3$  the ratio is  $(2.3 \pm 1.5) \times 10^{-11}$ . The preferred direction was within  $6^\circ$  of the earth's axis of rotation. The results for the  $P_3$  anisotropy are slightly larger than the  $1\sigma$  resolution of the apparatus and could represent an anisotropy. However, the systematic effects discussed below are more probably the cause.

Most systematic effects are fixed relative to the laboratory and appear to rotate with the earth when viewed from the celestial sphere. It is easy to differentiate these systematic effects from anisotropies which are fixed relative to the celestial sphere. However, any component of a systematic effect along the axis of the earth's rotation appears fixed relative to the celestial sphere. Hence, such a systematic effect would show up, in the analyzed data, as a spurious anisotropy directed toward the pole star.

At a lower sensitivity, a systematic effect with three-fold symmetry was discovered and remedied by changing the design of the bearing blocks. Initially, the vacuum-chamber base and interferometer rolled upon three bearings. These bearings were fixed in the laboratory. As the apparatus was rotated, the vacuum chamber base was periodically deformed by the bearings. This deformation was transmitted to the interferometer base and caused the mirror mounts to distort in such a manner that a threefold anisotropy was observed in the data taken with the apparatus. The resolution of the problem was to attach the bearing blocks to the vacuum chamber base. Even though the vacuum chamber base is still distorted by the force required to support the apparatus, this force is now always on the same points of the vacuum chamber base, and the base does not change its distortion as the apparatus is rotated. This reversal of the bearing blocks eliminated the threefold anisotropy observed in the data at the earlier level of sensitivity.

In the final data analysis, an anisotropy of threefold symmetry is observed that is almost two orders of magnitude smaller than the earlier anisotropy described above. One possible mechanism for this smaller effect is as follows. The bearings gradually wear a shallow track in the phosphor bronze sheet that the apparatus rolls on. Since the bearings are free to wander slightly, they can wear an irregular track. If there is one area where the wandering is extreme, every time one

of the three bearings rolls over this area, a force is transmitted to the vacuum chamber base. This could distort the interferometer and cause a smaller three-fold anisotropy in the data.

Although the ether wind velocity has been shown to be less than 1/1000 the orbital velocity of the earth<sup>4</sup> and, hence, physically improbable, it is still interesting to consider whether the interferometer described in this paper can detect the ether wind. In publishing the results of their experiment, Michelson and Morley quote Fresnel on the believed behavior of the index of refraction in an ether wind:

On the undulatory theory, according to Fresnel, first, the ether is supposed to be at rest except in the interior of transparent media, in which secondly, it is supposed to move with a velocity less than the velocity of the medium in the ratio  $(n^2 - 1)n^{-2}$ , where  $n$  is the index of refraction. These two hypotheses give a complete and satisfactory explanation of aberration. The second hypothesis, notwithstanding its seeming improbability, must be considered as fully proved, first, by the celebrated experiment of Fizeau, and secondly, by the ample confirmation of our own work.<sup>5</sup>

The above quotation refers to the Fresnel dragging coefficient. If the glass moves at velocity  $\vec{v}_e$  relative to the general ether frame, then the ether within the glass is dragged enough so that it moves at velocity  $\vec{v}_e(n^2 - 1)n^{-2}$  relative to that general frame. Our concern is with the velocity of light in the glass as seen by an observer stationary with respect to the glass; call this  $\vec{c}_g$ . This velocity can be expressed as a sum: the velocity of light relative to the dragged ether plus the velocity of the dragged ether relative to the glass. The former is, one assumes, the standard vacuum value divided by the refractive index,  $\vec{c}_0/n$ . The latter can be written as the difference in the velocities of the dragged ether and the glass relative to the general ether frame. Thus one has

$$\vec{c}_g = \frac{\vec{c}_0}{n} + \left[ \left( \frac{n^2 - 1}{n^2} \right) \vec{v}_e - \vec{v}_e \right], \quad (12)$$

$$\vec{c}_g = \frac{\vec{c}_0}{n} - \frac{1}{n^2} \vec{v}_e. \quad (13)$$

To determine the magnitude of  $\vec{c}_g$  as a function of direction, one squares both sides, expands the right-hand side of first order in  $\vec{v}_e/c_0$  and when

taking the square root, finds

$$\begin{aligned} c_g &\simeq c_0 n^{-1} [1 - (\vec{v}_e \cdot \vec{c}_0)(c_0^2 n)^{-1}] \\ &\simeq c_0 n^{-1} [1 - (v_e/n) c_0^{-1} \cos \phi]. \end{aligned} \quad (14)$$

Here  $\phi$  is the angle between the direction of light propagation and the velocity of the glass relative to the general ether frame, that is,  $\cos \phi = \vec{c}_0 \cdot \vec{v}_e / |\vec{c}_0| v_e$ . The anisotropy shown in Eq. (14) has the same form as the  $P_1$  anisotropy and can therefore be detected by this experiment. This experiment sets an upper limit to the ether wind of  $(v_e/c_0) = (0.015 \pm 1.3) \times 10^{-10}$ . The uncertainty in  $v_e$  is less than 3.8 cm/sec, which is  $1.3 \times 10^{-6}$  of the orbital velocity of the earth.

## V. CONCLUSION

A triangular interferometer is used to detect anisotropies in the phase velocity of light. Anisotropies can be detected that behave as the first ( $\cos \phi$ ) and third ( $\frac{5}{2} \cos^3 \phi - \frac{3}{2} \cos \phi$ ) Legendre polynomials. The  $\phi$  is the angle between a single preferred direction in space and the direction of light propagation. The results of this experiment are expressed as an upper limit for the anisotropy in the speed of light, divided by the speed of light. For the anisotropy that behaves as the first Legendre polynomial, this ratio is  $(0.1 \pm 8.4) \times 10^{-11}$ , and for the third Legendre polynomial this ratio is  $(2.3 \pm 1.5) \times 10^{-11}$ . A piece of glass is used in the interferometer for the analysis of the first Legendre polynomial. In this analysis it is assumed the index of refraction is a constant that does not depend on the direction in which the light is propagating.

If one assumes, as did Michelson and Morley, the Fresnel dragging coefficient describes the motion of ether in glass, this experiment can also be interpreted as an ether wind experiment. If  $v_e$  is the ether velocity at the surface of the earth, the ratio of  $v_e$  to the speed of light is less than  $(0.015 \pm 1.3) \times 10^{-10}$ .

## ACKNOWLEDGMENT

Conversations with many people have been helpful in formulating and interpreting this experiment. The authors would especially like to thank Dr. Kevin Cahill, Dr. William L. Trousdale, and Dr. Bruce W. Hawkins.

\*Part of a thesis submitted by one of us (W.S.N.T.) to Wesleyan University in partial fulfillment of the requirements for a Ph.D. degree in physics.

†First presented at the American Physical Society meeting, Washington, D. C., April 1972.

‡Present address: The College of Wooster, Wooster, Ohio 44691.

§Present address: Joint Institute of Laboratory Astrophysics, Boulder, Colorado 80302.

||Present address: University of Arizona, Tucson,

Arizona 85721.

<sup>1</sup>W. Trimmer and R. Baierlein, following paper, Phys. Rev. D **8**, 3326 (1973).

<sup>2</sup>A. J. Montgomery, J. Opt. Soc. Am. **57**, 1121 (1969).

<sup>3</sup>K. C. Turner and H. A. Hill, Phys. Rev. **134**, B252

(1964).

<sup>4</sup>T. S. Jaseja, A. Javan, J. Murray, and C. H. Townes, Phys. Rev. **133**, A1221 (1964).

<sup>5</sup>A. A. Michelson and E. W. Morley, Am. J. Sci. Third Series **34**, 22 (1887).

PHYSICAL REVIEW D

VOLUME 8, NUMBER 10

15 NOVEMBER 1973

## Anisotropic Modification of Maxwell's Equations

William S. N. Trimmer\* and Ralph F. Baierlein

*Wesleyan University, Middletown, Connecticut 06457*

(Received 9 April 1973)

This paper examines a modified form of Maxwell's equations, one designed to produce anisotropic light propagation in a vacuum. The equations predict anisotropies in the speed of light that behave as  $\cos \phi$  and  $\cos 2\phi$ , where  $\phi$  is the angle between the actual direction of propagation and some single preferred direction in space. The predicted index of refraction also has terms that behave as  $\cos \phi$  and  $\cos 2\phi$ .

### I. INTRODUCTION

In the preceding paper,<sup>1</sup> we discussed an experiment designed to measure anisotropies in the speed of light. It is difficult to use Maxwell's equations to justify the assumptions made in the earlier paper because Maxwell's equations do not predict an anisotropy in the speed of light in a vacuum. This paper will examine a modified form of Maxwell's equations which predict an anisotropy of interest. The index of refraction, phase velocity, and optical path length will be discussed.

### II. THE OPTICAL PATH LENGTH

In Ref. 1 the extra optical path length due to a piece of glass was used to search for an anisotropy in the speed of light. This anisotropy has the form  $c(\phi) = c_0(1 + b_1 \cos \phi)^{-1}$ , where  $c(\phi)$  is the vacuum phase velocity of light,  $c_0$  is a constant,  $b_1$  is a small number which determines the size of the anisotropy, and  $\phi$  is the angle between the actual direction of light propagation and some single preferred direction  $\hat{\mu}$ . The interferometer used always passes the light through exactly the same portion of the glass. The entire interferometer is periodically rotated, however, and it is possible that the index of refraction,  $n(\phi)$ , might change due to the rotation of the glass. If the index changes in a perverse manner, the change could just cancel the effect due to the  $\cos \phi$  anisotropy. To examine what this perverse form is, consider the optical path length,  $L_{o.p.}$ ,

$$L_{o.p.} = \int_A^D \lambda^{-1} dl. \quad (1)$$

$L_{o.p.}$  is the number of wavelengths contained in the optical path between points  $A$  and  $D$ . When one uses the fundamental relationship

$$\begin{aligned} \lambda \nu &= \frac{c(\phi)}{n(\phi)} \\ &= \text{phase velocity}, \end{aligned} \quad (2)$$

Eq. (1) becomes

$$L_{o.p.} = \int_A^D \nu n(\phi) [c(\phi)]^{-1} dl. \quad (3)$$

In these equations  $\lambda$  is the wavelength, and  $\nu$  is the frequency of the monochromatic light under consideration. Now if glass is present, the index of refraction can be written as its vacuum value, 1, plus a term due to the glass,  $g(\phi)$ :

$$n(\phi) = 1 + g(\phi). \quad (4)$$

Equation (3) now becomes

$$L_{o.p.} = \int_A^D \nu [c(\phi)]^{-1} 1 dl + \int_A^D \nu [c(\phi)]^{-1} g(\phi) dl. \quad (5)$$

The anisotropy in the first term integrates to zero (to first order in  $b_1$ ) when the integral is over a closed path, as pertains to most interferometers (see Sec. II of Ref. 1). The second integral is non-zero only over the portions of the path containing glass. Unless  $g(\phi)$  has exactly the same form as  $c(\phi)$ , the second integral can be arranged so it has